SYNERGISTIC EFFECT OF Pd+Rh ON THE MICROSTRUCTURE AND OXIDATION RESISTANCE OF ALUMINIDE COATINGS

M. Zagula-Yavorska

Rzeszów University of Technology, Department of Materials Science, Faculty of Mechanical Engineering and Aeronautics, Rzeszów, Poland

Abstract

The Pd+Rh modified aluminide coatings were deposited on nickel and CMSX-4 nickel superalloy. The Pd layer (2.5 µm thick) and the subsequent Rh layer (0.5 µm thick) were electroplated on both nickel and CMSX-4. The aluminization of the substrates with Pd+Rh layers was carried out using the CVD method. Two zones (outer and interdiffusing) were observed on both coatings. The β-NiAl phase doped in palladium was formed in the outer zones and β-NiAl phase doped with palladium and rhodium was formed at the boundary between the outer and interdiffusion zones of both coatings. The γ'-Ni_3Al phase and µ-Co_7Mo_6 precipitates in the β-NiAl matrix were found in the interdiffusion zone on nickel and CMSX-4 superalloy respectively. The simultaneous use of Pd and Rh in the aluminide coating slowed down their oxidation rate. Moreover, Pd+Rh co-doping is more efficient than Pd+Hf in reducing the oxidation rate of aluminide coating on CMSX-4 superalloy.

Keywords: Pd+Rh; Aluminide coating; Oxidation; k_p value

1. Introduction

Turbine engines are made of Ni-based superalloys [1]. Low aluminium content in superalloys is a reason of their poor hot corrosion resistance and fast oxidation at service temperature. As a result, the lifetime of engines has been shortened [1]. Therefore, aluminide coatings were applied in turbine engines to improve their high temperature oxidation resistance and hot corrosion resistance [2]. Aluminide coatings are commonly used in turbine engines due to their low cost and slow oxidation. Unfortunately, oxidation of aluminide coatings causes their degradation through internal weakening and deformation. Slowing down of the oxide layer growth and improvement of oxides adherence to the coating are necessary to rise oxidation resistance of coatings [3]. Platinum in aluminide coatings: 1) improves oxide layer adhesion during oxidation; 2) reduces voids growth at the oxide layer-coating interface during oxidation; 3) mitigates detrimental sulfur effects on oxide layer adhesion; 4) accelerates Al_2O_3 oxide re-growth after spallation; 5) prevents Ta-rich secondary oxides formation [4].

Tolpygo and Clarke [5] revealed that platinum modified aluminide coatings degraded by rumpling. Small temperature decrease during oxidation cycle (even 100 ºC) was sufficient to rumpling of the platinum modified aluminide coatings. Tolpygo and Clarke [5] alleged that rumpling was a result of the thermal expansion mismatch between the superalloy and the modified coating and was driven by the plastic deformation of the thermally grown oxide and the coating.

Palladium has many chemical similarities to platinum [6]. Palladium addition to the aluminide coatings facilitates the θ-Al_2O_3 to α-Al_2O_3 oxide transition and accelerates titanium diffusion from the superalloy substrate to the coating [7]. Palladium stabilizes the β-(Ni,Pd)Al phase in the coating and impends outward diffusion of elements from substrate to the coating which delays its degradation. Palladium both stabilizes the alumina oxide and significantly decreases hot corrosion of the coating [8]. Sufficient amount of rhodium in the Ni-base alloy can substantially improve the performance of the α-Al_2O_3 oxide that forms during alloy exposure at elevated temperature [9]. Currently, modification of coating by two elements is applied to prolong lifetimes of coated elements [10]. The Pt and Pd modified aluminide coatings were considered as economically alternative for the Pt modified ones [11]. Pt and Pd were distributed on the upper layer of the coating and their amount decreased inward the coating. The course of oxidation of Pt and Pd modified coatings was different from the Pt modified or non-modified ones. Pt and Pd modified aluminide coatings exhibited better cyclic oxidation resistance than Pt modified, non-modified or Pd modified ones

[11]. The β-NiAl phase was more stable, moreover α-Al_2O_3 oxide maintained longer than on the other modified coatings during oxidation [12]. The Pt and Pd modified coating picked up 25 % more aluminum than Pt modified one, resulting in the best resistance to oxidation [7]. Rhodium and hafnium modified coating exhibited better oxidation resistance compared to those modified only with rhodium [13]. Rhodium dissolved in the β-NiAl phase, while hafnium formed Hf-rich precipitations in the β-(Ni,Rh)Al phase. Hf-rich particles blocked the diffusion of the aluminum and the substrate elements, whereby oxidation of coating was slow [14].

Using more than one modificators (Pt+Pd, Pt+Hf, Pd+Hf or Rh+Hf) in coatings can significantly prolong the coated superalloy lifetime [10-15]. Therefore, synergistic effect of Pd+Rh influence on the microstructure and oxidation kinetics of aluminide coatings will be analyzed. The synergistic effect of this pair of modificators has not been investigated yet.

2. Materials and methods

Pure nickel and CMSX-4 Ni-based single crystal superalloy were used as the substrates. The composition of the superalloy was [wt. % 61.5Ni, 6.5Cr, 0.6Mo, 6.5Ta, 5.6Al, 1Ti, 9Co, 6W, 0,1Hf, 3Re]. The samples of pure nickel and superalloy (12 mm diameter, 5 mm thick) were polished with #320, 500, 800 and 1000 emery paper and cleaned in ethanol for 5 min. The 2.5 μm of Pd + 0.5 μm of Rh layers were electroplated. Palladium layers (2.5 μm thick) were deposited electrochemically first and rhodium layers (0.5 μm thick) were deposited subsequently. Then, samples were aluminized by the CVD method [16]. The BPXPR0325S equipment produced by the IonBond Company was used [17]. The aluminide coating deposition process consisted of: heating of the electroplated samples from 20 ˚C up to 1040 ˚C and aluminizing at 1040 ˚C for 720 min. Then samples with palladium and rhodium modified aluminide coatings were cut, grinded and polished. Microareas' chemical composition and cross-section element distribution were investigated by the X-ray energy dispersive spectrometry (EDS) (INSPECT F50). Phase composition of the modified coating was identified by X-ray diffractometer (XRD) (ARL X'TRA X-ray diffractometer equipped with a filtered copper lamp with the voltage of 45 kV was used) and by electron back scatter diffraction (EBSD) (INSPECT F50). The oxidation resistance of palladium and rhodium modified aluminide coating on CMSX-4 superalloy was analyzed by oxidizing in air at 1100 °C for 20 hours and next cooling to room temperature for 2 hours. The coated samples were inspected and weighted after each cycle of oxidation. The oxidation kinetics of the palladium and rhodium modified aluminide coating were compared with the palladium modified one (3 μm Pd thick) on the CMSX-4 superalloy.

3. Results
3.1. Palladium and rhodium modified aluminide coating on nickel

The cross-section microstructure was presented in Fig. 1a. The EDS spectrum in micro-areas was shown in Fig. 1b-f. The coating exhibited a zonal structure comprising of ~ 46 μm thick outer zone and ~8 μm thick interdiffusion zone situated on the substrate. The aluminium composition in the top of the outer zone (Table 1) indicated that the coating grew rather by nickel diffusion from the substrate than aluminium diffusion from the gas phase to the substrate. Such a structure was typical for aluminide coatings deposited by low activity aluminizing process [18]. The chemical composition obtained of the outer zone of the coating suggested the presence of the palladium doped β-NiAl phase that contained 42.8 at.% Al and 57.1 at.% Ni and small Pd content (Table 1). There was no Rh on the top of the outer zone of the coating (Fig. 1 b). The middle of the outer zone of the coating contained 40.1 at.% Al and 59.7 at.% Ni and ~ 0.2 at.% Pd (Table 1), suggesting the presence of the palladium modified β-NiAl phase. There was no Rh in the middle of the outer zone of the coating (Fig. 1c). The bottom of the outer zone contained 38.4 at.% Al, 61.0 at.% Ni, ~ 0.4 at.% Pd and ~ 0.4 at.% Rh (Table 1), suggesting the presence of the palladium and rhodium doped β-NiAl phase. Neither Pd nor Rh was found in the interdiffusion zone (Table 1). The interdiffusion zone contained only 26.5 at.% Al and 73.5 at.% Ni. It corresponded to the γ'-Ni_3Al phase according to Al-Ni phase diagram [19-24]. Cross-section concentration profiles of elements are presented in Fig. 2. The Al concentration decreased inward the coating, while Ni concentration decreased outward the coating (Fig. 2). The line scan of EDS in Figure 2 showed that Rh and Pd were distributed in the NiAl outer layer. Palladium was evenly distributed in the outer zone, while Rh was mainly located on the bottom of the outer zone (Fig. 2). The Rh content was ±0.1 % at. in the interdiffusion zone as well in the top and middle part of the outer zone (Fig. 2). Such Rh content was within the margin of error. XRD pattern contained peaks of the β-NiAl phase (Fig. 3).

3.2. Palladium and rhodium modified aluminide coating on the single crystal superalloy

The cross-section microstructure was presented in Fig. 4a. The EDS spectrum in micro-areas of the coating was shown in Fig. 4b-e. Two distinctive zones
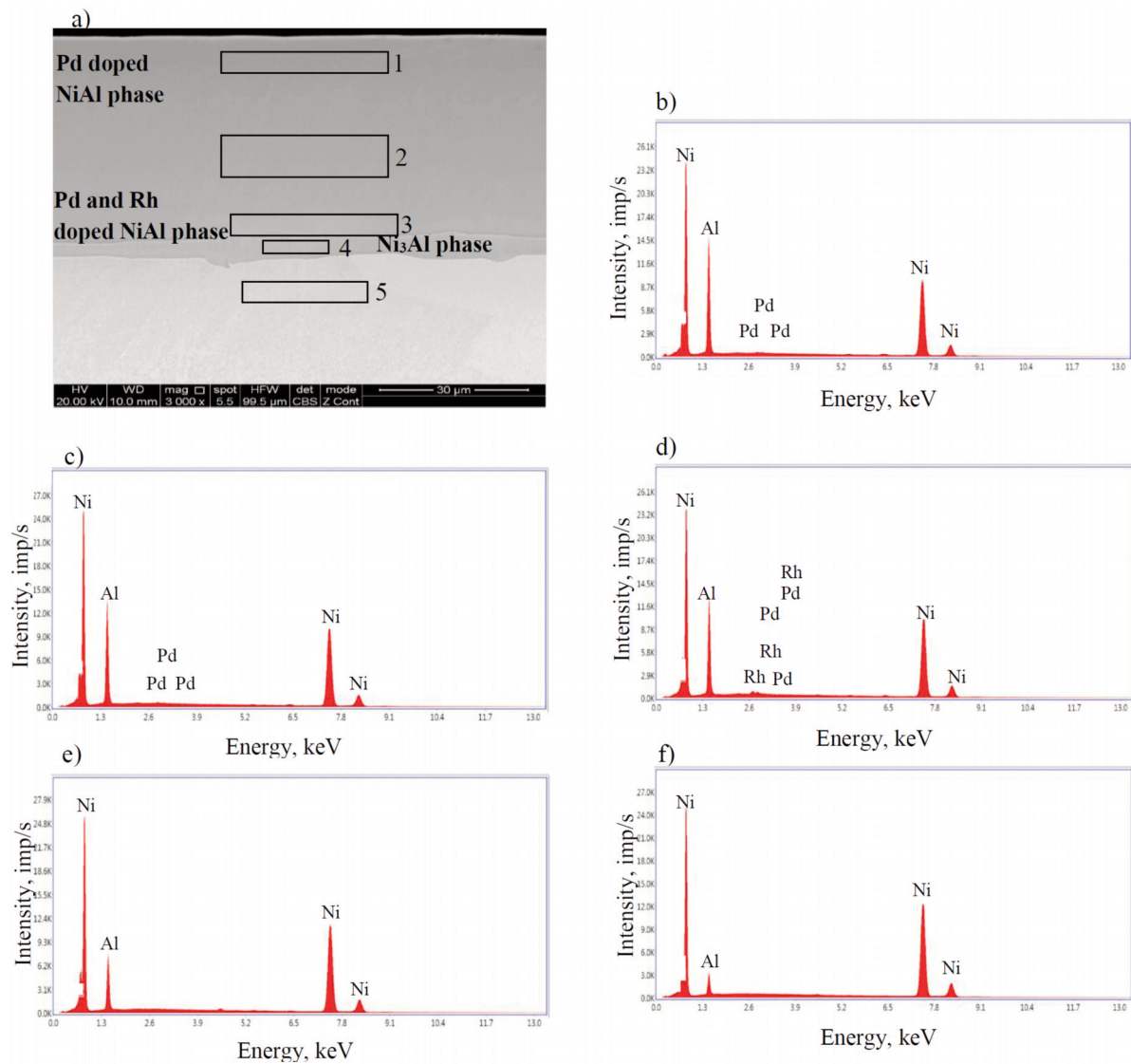
Figure 1. *Cross-section microstructure of the palladium and rhodium modified aluminide coating on pure nickel (a) and EDS spectrum of the top of the outer zone (b), middle of the outer zone (c), bottom of the outer zone (d), interdiffusion zone (e) and substrate border (f)*

Table 1. *Cross-section chemical composition of the palladium and rhodium modified aluminide coating on pure nickel*

Micro-area		Chemical composition, at.%			
		Al	Ni	Pd	Rh
1	Top of the outer zone	42.8±3.4	57.1±1.1	0.1±0	-
2	Middle of the outer zone	40.1±3.2	59.7±1.2	0.2 ±0.1	-
3	Bottom of the outer zone	38.4±3.1	61.0±1.2	0.4±0.1	0.2±0.1
4	Interdiffusion zone	26.5±2.2	73.5 ±1.4	-	-
5	Substrate border	12.3±1.1	87.7±1.7	-	-
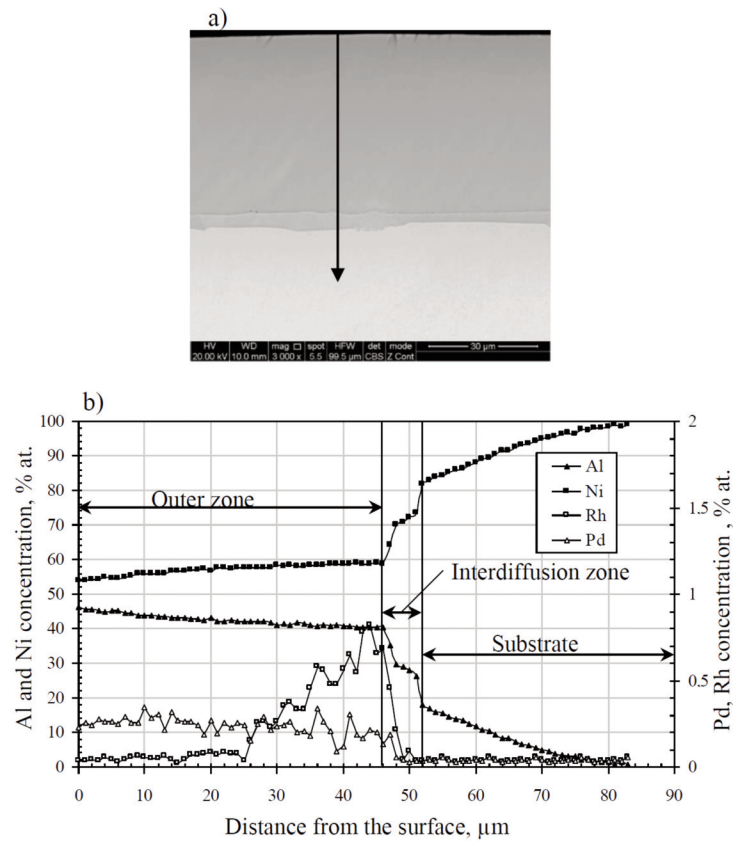
Figure 2. Microstructure (a) and cross-section concentration profiles (b) of aluminium, nickel, palladium and rhodium in the palladium and rhodium modified aluminide coating on pure nickel
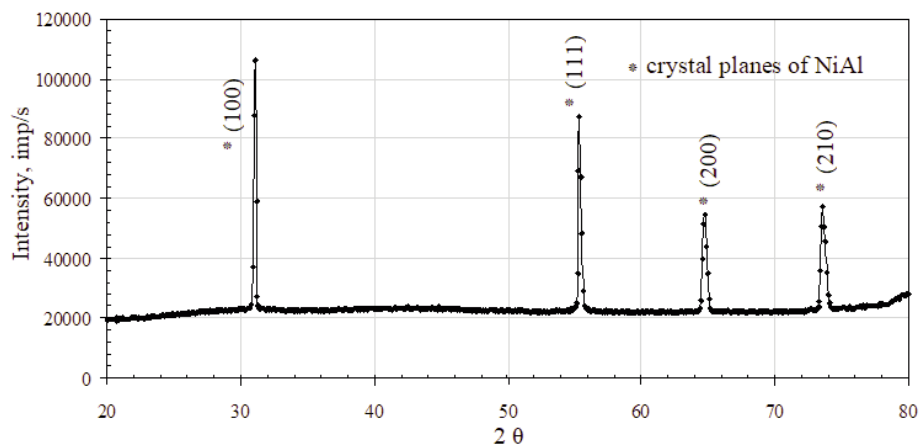
Figure 3. XRD pattern of the palladium and rhodium modified aluminide coating on pure nickel

are visible: the outer zone (~15 μm thick) and the interdiffusion one (~19 μm thick). The chemical composition analysis of the top of the outer zone of the coating suggested the presence of the palladium doped β-NiAl phase, which contained 42.6 at.% Al, 51.0 at.% Ni and 0.3 at.% Pd (Table 2). There was no Rh in the top of the outer zone (Fig. 4b). The bottom of the outer zone contained 37.6 at.% Al, 51.3 at.% Ni, ~ 0.4 at.% Pd and ~ 0.4 at.% Rh (Table 2),

suggesting the presence of the palladium and rhodium doped β-NiAl phase. The top of the interdiffusion zone contained 35.9 at.% Al, 51.2 at.% Ni, ~ 0.3 at.% Pd and ~ 0.6 at.% Rh (Table 2), suggesting the presence of the palladium and rhodium doped β-NiAl phase. Neither Pd nor Rh was found in the middle of the interdiffusion zone. The higher content of the refractory elements: Cr, Co, Ta and W in the middle of the interdiffusion zone than in the top and bottom of

the outer zone and than in the top of the interdiffusion zone of the coating was revealed. Moreover, Re and Mo appeared in the middle of the interdiffusion zone. Cross-section concentration profiles of elements were presented in Fig. 5. Nickel concentration decreased outward the coating, while Al concentration decreased inward the coating (Fig. 5). Palladium was evenly distributed in the outer zone. Palladium and rhodium were located on the bottom of the outer zone and on the top of the interdiffusion zone (Fig. 5). There was no Rh both in the interdiffusion zone as well as in the

top and middle part of the outer zone, similarly as on pure nickel. In the interdiffusion zone, at a depth of 14 μm, there was the rise of the Cr and Re content. XRD pattern contained peaks of β-NiAl phase and μ-Co_7Mo_6 phase (Fig. 6). The EBSD analysis results revealed the β-NiAl phase in the outer zone (Fig. 7a-c). This confirmed the results obtained by XRD from the surface of the coating. The μ-Co_7Mo_6 precipitates distributed in the β-NiAl phase of the interdiffusion zone were identified (Fig. 7d-i).
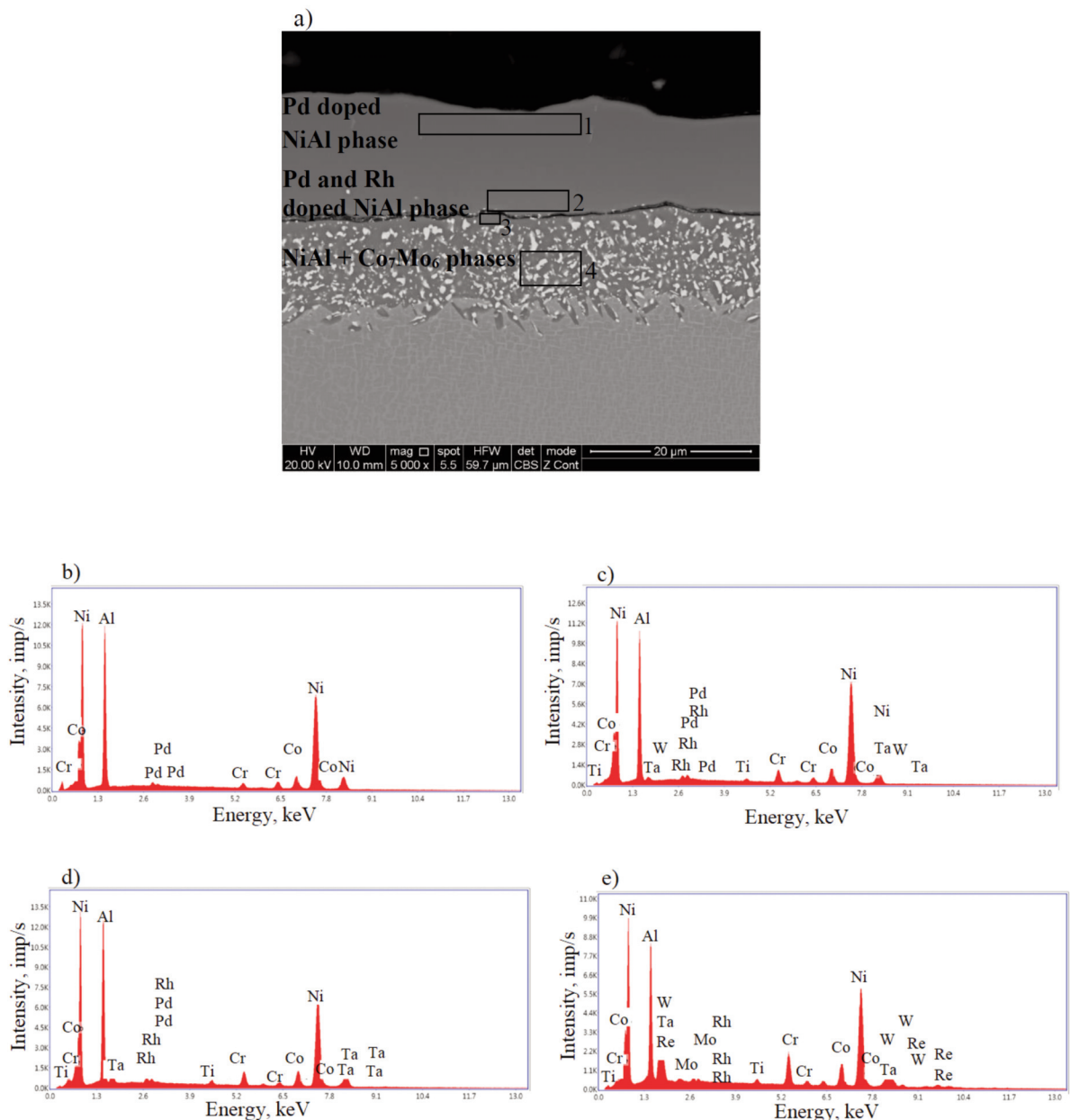
Figure 4. Cross-section microstructure of the palladium and rhodium modified aluminide coating on CMSX-4 superalloy (a) and EDS spectrum of the top of the outer zone (b), bottom of the outer zone (c), top of the interdiffusion zone (d) and middle of the interdiffusion zone (e)

Table 2. *Cross-section chemical composition of the palladium and rhodium modified aluminide coating on CMSX-4 superalloy*

	Microarea	Chemical composition , at.%										
		Al	Mo	Rh	Pd	Ti	Cr	Co	Ni	Ta	W	Re
1	Top of the outer zone	42.6±3.4	-	-	0.3±0.1	-	1.2±0.1	4.9±0.2	51.0±1.0	-	-	-
2	Bottom of the outer zone	37.6±3.0	-	0.4±0.1	0.4±0.1	0.5±0.1	2.9±0.2	6.1±0.2	51.3±1.1	0.4±0.1	0.4±0.1	-
3	Top of the interdiffusion zone	35.9±2.9	-	0.6±0.1	0.3±0.1	1.0±0.1	3.6±0.2	6.6±0.2	51.2±1.1	0.8±0.2	-	-
4	Middle of the interdiffusion zone	22.6±1.8	0.4±0.1	-	-	0.8±0.1	11.3±0.4	10.9±0.4	41.6±1.2	2.1±0.4	7.3±0.6	3.0±0.4

a)

b)
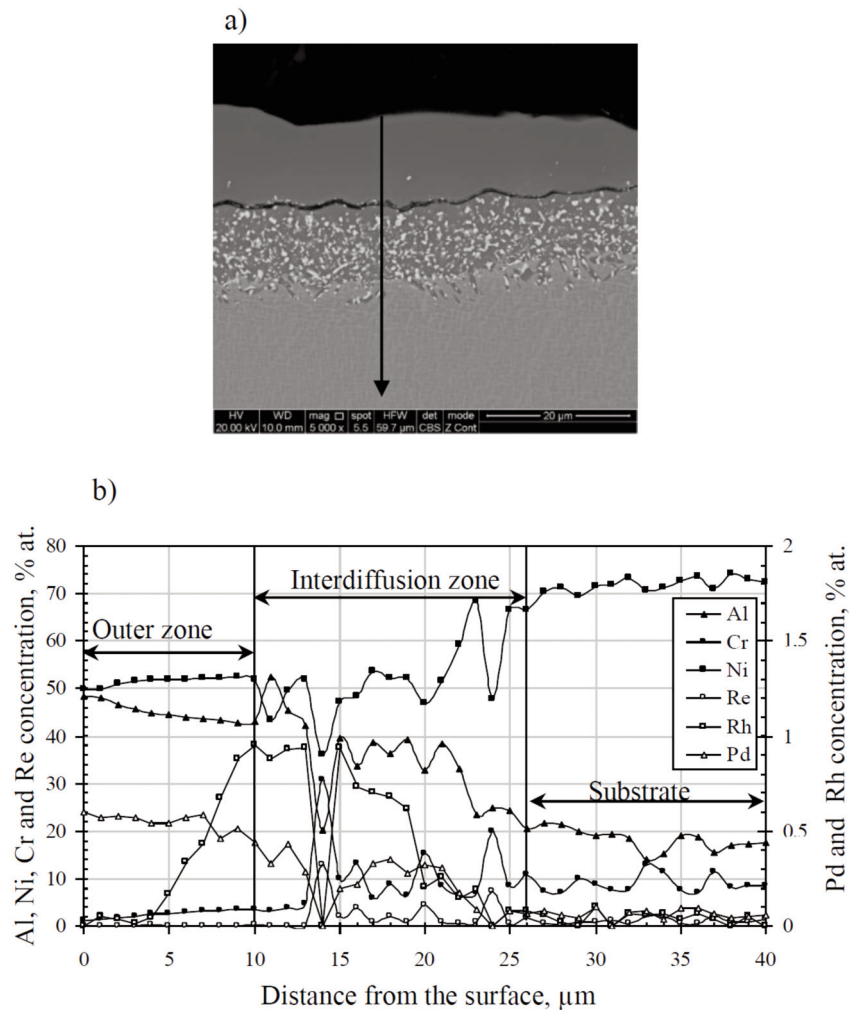
Figure 5. *Microstructure (a) and cross-section concentration profiles (b) of aluminium, nickel, chromium, rhenium, palladium and rhodium in palladium and rhodium modified aluminide coating on CMSX-4 superalloy*
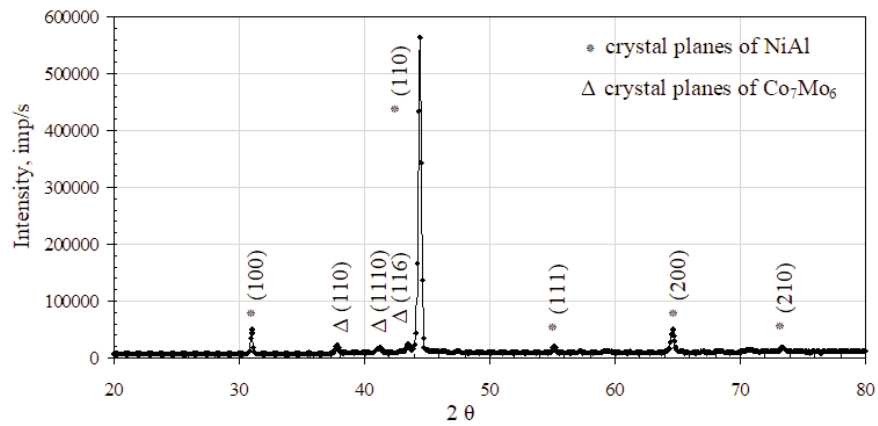
Figure 6. XRD pattern of the palladium and rhodium modified aluminide coating on CMSX-4 superalloy
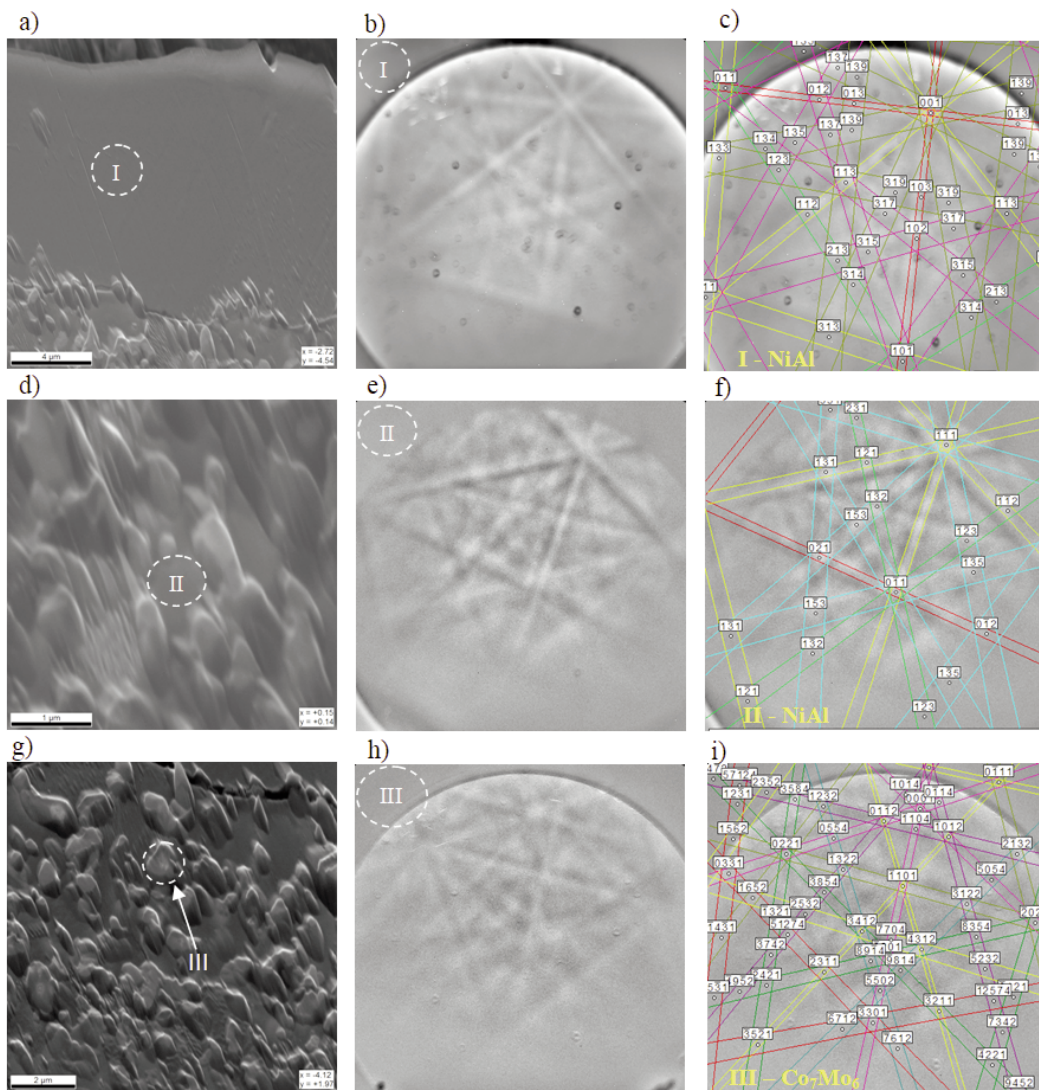
Figure 7. EBSD results: for NiAl phase in the outer zone I (a-c), Kikuchi pattern (b), corresponding indexes (c); for NiAl phase in the interdiffusion zone II (d-f), Kikuchi pattern (e), corresponding indexes (f) and for Co₇Mo₆ phase in the interdiffusion zone III (g-i) Kikuchi pattern (h), corresponding indexes (i) of the palladium and rhodium modified aluminide coating on CMSX-4 superalloy

3.3. Oxidation resistance of the palladium and palladium and rhodium modified aluminide coating on CMSX-4 superalloy

Oxidation kinetics curves of the palladium and palladium and rhodium modified aluminide coatings on CMSX-4 superalloy were presented in Fig. 8. Both coatings initially exhibited a weight growth (Fig. 8). Double modified one exhibited weight growth during the first 80 h of oxidation. This was due to the oxide layer formation. Then, from 20 h to 80 h the weight growth of the double modified coating was slow. This was caused by oxide layer spallation and re-formation. From 80 h to 150 h of oxidation the weight change of the palladium and rhodium modified aluminide coating was stable. This was due to the presence of the dense protective oxide layer. Then, after 150 h the weight of the double modified coating raised. This could be caused by oxide layer spallation and re-formation.

Single modified coating exhibited fast weight growth during the first 20 h of oxidation. This, as above, could be due to the oxide layer formation. From 20 h to 40 h the weight growth of the single modified coating was subtle, which was caused by oxide layer formation and its spallation. From 40 h to 170 h the weight decreased. That could be related to faster oxide layer spallation than re-formation. Therefore palladium modified aluminide coating exhibited worse oxidation resistance than those modified by palladium and rhodium (Fig. 8).

The constant k_p value of the palladium and rhodium modified aluminide coating oxidation rate was established by the slope of the matched line, was 6×10^{-4} mg^2/cm$^4 \cdot$h (Fig. 9).

4. Discussion

Palladium and rhodium modified aluminide coatings were deposited on nickel and CMSX-4 superalloy. Two zones (outer and interdiffusion zone) were observed on both substrates. Similar structure was observed for hafnium or zirconium modified aluminide coatings deposited on nickel and
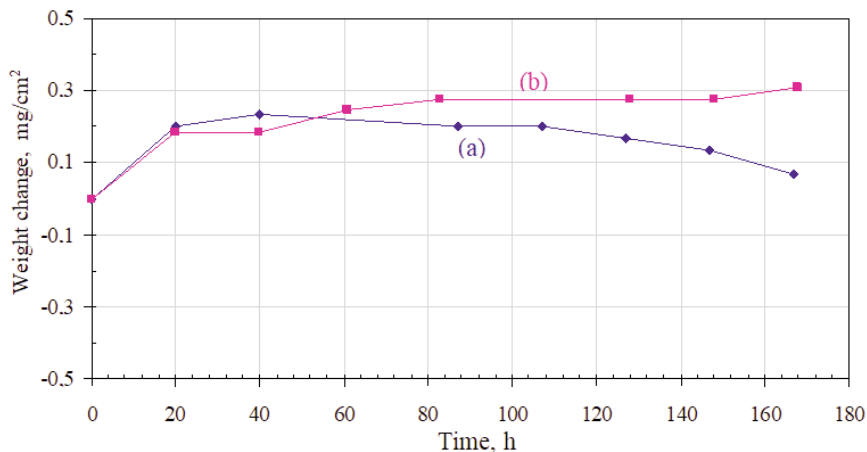
Figure 8. *Oxidation behaviour of the palladium (a) and palladium and rhodium (b) modified aluminide coating on CMSX-4 superalloy*
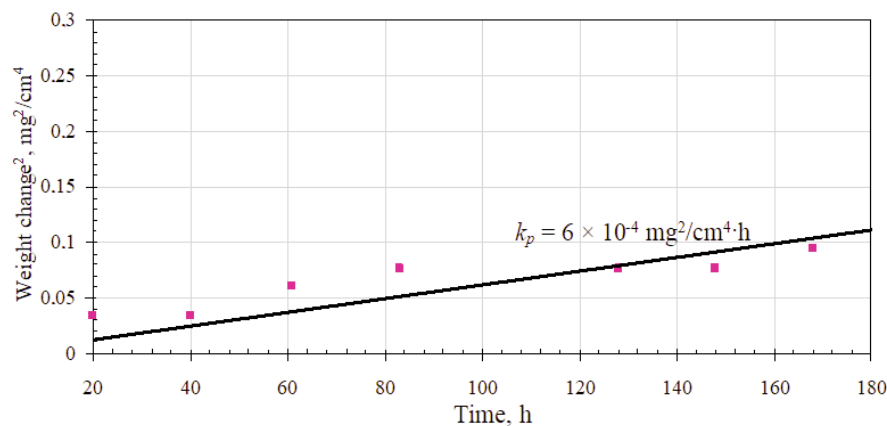
Figure 9. *Weight change square versus oxidation time of the palladium and rhodium modified aluminide coating on CMSX-4 superalloy*

superalloys [25-27]. The palladium doped β-NiAl phase was on the top of the outer zone and palladium and rhodium doped β-NiAl phase was on the bottom of outer zone of both substrates. The interdiffusion zone on the nickel substrate consisted of the γ'-Ni$_3$Al phase. The β-NiAl phase was identified as a matrix of the interdiffusion zone on CMSX-4 substrate. The fine precipitates of the rhombohedral μ-Co$_7$Mo$_6$ phase in the β-NiAl phase of interdiffusion zone were identified. Such precipitates were also identified by Pillai et al. [28] in the interdiffusion zone of aluminide coating. Rejection of Co and Mo from the superalloy substrate and their low solubility in the β-NiAl phase lead to Co$_7$Mo$_6$ phase precipitation in the β-NiAl phase [3, 29]. Kirkendall-like porosity was observed between the outer and interdiffusion zones (Fig. 4). Kirkendall-like pores formed because of the unbalanced diffusion of elements into and out of the alloy. According to Kirkendall–Frenkel theory, there was an unbalanced flow of nickel and aluminum atoms in the diffusion zone. The value of nickel diffusion coefficient was bigger than aluminum ($D_{Ni} > D_{Al}$). The unbalanced flux of nickel and aluminum atoms resulted in the differences in microvolume and caused stress in the interdiffusion zone. The microvolume was reduced in the area of higher nickel concentration and vacancies were formed. When the number of vacancies were big, vacancies coagulated, pores were formed and Kirkendall porosity was generated [26].

Palladium was distributed over the outer zone on both nickel and CMSX-4 superalloy substrates. Palladium content in the outer zone on nickel substrate was about 0.1-0.4 at. %, while on CMSX-4 superalloy was about 0.4-0.6 at. %. This was less than palladium solubility in the β-NiAl phase (over 15 at. %) [30, 31]. This indicated that palladium was fully dissolved in the β-NiAl phase. Small rhodium content < 1 at. % was found at the outer/interdiffusion zone border both on the nickel and CMSX-4 superalloy substrates. This content was such small that rhodium was fully dissolved in the β-NiAl phase [32]. The atomic radiuses of Pd and Rh are 140×10^{-12} m and 135×10^{-12} m respectively. The atomic radius of Ni is 135×10^{-12} m. So Ni site in the β-NiAl phase crystal lattice may be occupied by Pd and Rh and the β-(Ni,Pd,Rh)Al could be formed at the outer/interdiffusion zone border. According to Hong et al. [7] a small content of Pd added to the Pt modified aluminide coating increased Ni diffusion from the substrate. The vacant sites for the Al, Pt and Pd diffusion were created. Al could diffuse easily to take up vacant sites in (Pt,Pd,Ni)Al. According to Lamesle et al. [32], the B2 structure of the palladium modified aluminide coating could be formed according to the reaction (1).

$$Pd_xNi_{1-x} + Al \rightarrow \left(Pd_xNi_{1-x}\right)Al\left(B2\ structure\right) \qquad (1)$$
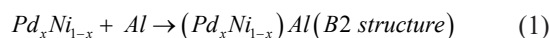
It is possible, that the B2 structure of the palladium and rhodium modified aluminide coating could be formed according to the reaction (2).

$$\left(Pd, Rh\right)Ni + Al \rightarrow \left(Pd, Rh, Ni\right)Al\left(B2\ structure\right) \qquad (2)$$
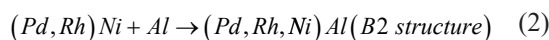
Neither Pd nor Rh was revealed in the middle of interdiffusion zone. It corresponded to results got by Swadźba et al. [11] for palladium and platinum modified aluminide coatings deposited on CMSX-4 superalloy. There was no rhodium in the top of the outer zone both on the nickel and CMSX-4 superalloy substrates. The melting point of Rh is significantly higher that those of Pd, Al and Ni, indicating that Rh has a higher activation energy of diffusion (Q), which is necessary for vibration of crystal lattice. A higher value of activation energy means that diffusivity (D) is lower (3) [14].

$$D = D_0 e^{-\frac{Q}{RT}} \qquad (3)$$

where D$_0$ is pre-exponential diffusion coefficient, R is the gas constant, T is temperature.

The diffusivity of Rh is smaller than Pd, therefore Rh was located only at the outer/interdiffusion zone border in contrast to Pd, which was located not only at the outer/interdiffusion zone border, but also diffused up to the coating.

The weight growth of the palladium and rhodium modified aluminide coatings on single crystal superalloy was about 0.3 mg/cm^2 after 170 h of exposure in the air atmosphere. This value is 0.05 mg/cm^2 smaller than the weight growth of the Hf modified β-(Ni,Pt)Al coating after 170 h of exposure in air [14]. This value is also 0.9 mg/cm^2 smaller than the weight growth of the Zr modified β-(Ni,Pt)Al coating after 170 h of oxidation [33].

The constant k$_p$ value of the palladium and rhodium modified aluminide coatings was about k$_p$ = 6 x 10^{-4} mg^2/cm^4·h. This was 1 x 10^{-4} mg^2/cm^4·h less than the k$_p$ value of the palladium and hafnium modified aluminide coatings on CMSX-4 superalloy [3].

The above results and its analysis indicated that the simultaneous usage of Pd+Rh in the aluminide coating slowed it oxidation rate. Moreover Pd+Rh was more efficient than Pd+Hf in reducing of the oxidation rate of aluminide coating on CMSX-4 superalloy.

5. Conclusion

A new kind of coating: Pd+Rh modified aluminide coating was deposited on nickel and CMSX-4

superalloy by first Pd layer electroplating (2.5 μm thick), second Rh layer electroplating (0.5 μm thick) and next aluminizing by the CVD method. Two zones (outer and interdiffusion) were observed in the palladium and rhodium modified aluminide coating both on nickel and CMSX-4 superalloy. The palladium doped β-NiAl phase on the top of the outer zone of both nickel and CMSX-4 superalloy was formed. Small rhodium and palladium content (< 1 at. %) was found at the outer/interdiffusion zone border both on the nickel and CMSX-4 superalloy substrates. Ni site in the β-NiAl phase crystal lattice could be occupied by the Pd and Rh. As a result, the β-(Pd,Rh,Ni)Al could be formed at the outer/interdiffusion zone border. The γ'-Ni$_3$Al phase and μ-Co$_7$Mo$_6$ precipitates in the β-NiAl matrix were found in the interdiffusion zone of nickel and CMSX-4 superalloy respectively. Neither Pd nor Rh was revealed in the middle of the interdiffusion zone. The simultaneous usage of Pd and Rh in the aluminide coating slowed its oxidation rate. The Pd+Rh modification was more efficient than Pd+Hf in reducing the oxidation rate of aluminide coating on CMSX-4 superalloy.

Author contributions

M. Zagula-Yavorska:
Conceptualization, Investigation, Methodology, Formal analysis, Writing– review & editing.

Conflict of interest

The author declare that they have no known competing financial interests or personal relationships that could have appeared to influence the work reported in this paper.

Ethical approval

This article does not contain any studies with human participants or animals performed by any of the authors. This study was done according to ethical standards.

Data availability

The data used to support the findings of this study are available from the corresponding author upon request.

References

[1] M. Zagula-Yavorska, J. Romanowska, The effect of precious metals in the NiAl coating on the oxidation resistance of the Inconel 713 superalloy, Journal of Mining and Metallurgy Section B-Metallurgy, 58 (2) (2022) 299-310.

https://doi.org/10.2298/JMMB220427011Z

[2] A. Kochmańska, P. Kochmański, Cyclic oxidation of slurry silicide-aluminide coatings formed on Ti-6Al-4V alloy, Surface Engineering, 39 (6) (2023) 738 – 750. https://doi.org/ 10.1080/02670844.2023.2257856

[3] J. Romanowska, J. Morgiel, Ł. Kolek, P. Kwolek, M. Zagula-Yavorska, Effect of Pd and Hf co-doping of aluminide coatings on pure nickel and CMSX-4 nickel superalloy, Archives of Civil and Mechanical Engineering, 18 (2018) 1421-1429. https://doi.org/10.1016/j.acme.2018.05.007.

[4] Y. Li, S. Li, C. Zhang, N. Xu, Z. Bao, Oxidation behavior and oxide transformation of a Pt-modified aluminide coating at moderate high temperature, Crystals, 11(8) (2021) 972. https://doi.org/10.3390/cryst11080972

[5] V.K. Tolpygo, D. R. Clarke, Rumpling of CVD (Ni,Pt)Al diffusion coatings under intermediate temperature cycling, Surface and Coating Technology, 203 (2009) 3278. https://doi.org/10.1016/j.surfcoat.2009.04.016

[6] E. Pauletti, A. Oliveira, The influence of Pd on the structure and oxidation performance of β-NiAl diffusion coatings, Materials research, (2023) 26:e20220384. https://doi.org/10.1590/1980-5373-MR-2022-0384

[7] S. J. Hong, G. H. Hwang, W. K. Han, S. G. Kang, Cyclic oxidation of Pt/Pd-modified aluminide coating on a nickel-based superalloy at 1150 °C, Intermetallics, 17 (2009) 381–386. https://doi.org/10.1016/j.intermet.2008.08.014

[8] L. Y. Qian, J. Wang, Y. S. Guo, H. Liu, Z. B. Bao, Influences of iridium and palladium on oxidation resistance of PtAl coating, Acta Metallurgica Sinica (English Letters), 34 (2021) 1120–1130. https://doi.org/10.1007/s40195-020-01185-y

[9] E. Felten, Use of platinum and rhodium to improve oxide adherence on Ni-8Cr-6Al alloys, Oxidation of Metals, 10 (1976) 23–28. https://doi.org/10.1007/BF00611696

[10] S. Li, M. Xu, C. Zhang, Y. Niu, Z. Bao, S. Zhu, et al., Co-doping effect of Hf and Y on improving cyclic oxidation behavior of (Ni,Pt)Al coating at 1150 ºC, Corrosion Science, 178 (2021) 109093. https://doi.org/10.1016/j.corsci.2020.109093

[11] R. Swadźba, M. Hetmańczyk, M. Sozańska, B. Witala, L. Swadźba, Structure and cyclic oxidation resistance of Pt, Pt/Pd-modified and simple aluminide coatings on CMSX-4 superalloy, Surface and Coating Technology, 206 (2011) 538-1544. https://doi.org/10.1016/j.surfcoat.2011.06.042

[12] R. Swadźba, M. Hetmańczyk, J. Wiedermann, L. Swadźba, G. Moskal, B. Witala, K. Radwański, Microstructure degradation of simple Pt, Pt+Pd-modified aluminide coatings on CMSX-4 superalloy under cyclic oxidation conditions, Surface and Coating Technology, 215 (2013) 16-23. https://doi.org/10.1016/j.surfcoat.2012.06.093

[13] M. Zagula-Yavorska, M. Wierzbińska, J. Sieniawski, Rhodium and hafnium influence on the microstructure, phase composition and oxidation resistance of aluminide coatings, Metals, 7 (2017) 1-11. https://doi.org/10.3390/met7120548

[14] Y. F. Yang, C. Y. Jiang, H. R. Yao, Z. B. Bao, S. L. Zhu, F. H. Wang, Preparation and enhanced oxidation performance of a Hf-doped single-phase Pt-modified

aluminide coating, Corrosion Science, 113 (2016) 17-25. https://doi.org/10.1016/j.corsci.2016.09.014

[15] Y. F. Yang, P. Ren, Z. B. Bao, S. L. Zhu, F. H. Wang, W. Li, Microstructure and cyclic oxidation of a Hf-doped (Ni,Pt)Al coating for single-crystal superalloys, Journal of Materials Science, 55 (2020) 11687–11700. https://doi.org/10.1007/s10853-020-04782-5

[16] M. Zagula-Yavorska, J. Morgiel, J. Romanowska, J. Sieniawski, Microstructure and oxidation behaviour investigation of rhodium modified aluminide coating deposited on CMSX 4 superalloy, Journal of Microscopy, 261 (2016) 320-325. https://doi.org/10.1111/jmi.12344

[17] M. Zagula-Yavorska, J. Romanowska, M. Pytel, J. Sieniawski, The microstructure and oxidation resistance of the aluminide coatings deposited by the CVD method on pure nickel and hafnium-doped nickel superalloys, Archives of Civil and Mechanical Engineering, 15 (2015) 862-872. https://doi.org/10.1016/j.acme.2015.03.006

[18] B. Karpe, K. Prijatelj, M. Bizjak, T. Kosec, Corrosion properties of aluminized 16Mo3 steel, Journal of Mining and Metallurgy Section B-Metallurgy, 59 (1) (2023) 91-100. https://doi.org/10.2298/JMMB220927008K

[19] H. Okamoto, Al-Ni (aluminum-nickel), Journal of Phase Equilibria and Diffusion, 25 (2004) 394. https://doi.org/10.1007/s11669-004-0163-0

[20] Y. Zhao, S. Cao, L. Zeng, et al., Intermetallics in Ni–Al Binary Alloys: Liquid Structural Origin, Metallurgical and Materials Transactions A, 54 (2023) 646–657. https://doi.org/10.1007/s11661-022-06910-z

[21] P. Sankanit, V. Uthaisangsuk, P. Pandee, Tensile properties of hypoeutectic Al-Ni alloys: Experiments and FE simulations, Journal of Alloys and Compounds, 889 (2021) 161664. https://doi.org/10.1016/j.jallcom.2021.161664

[22] V.V. Kulyk, O.P. Ostash, V.V. Vira, Influence of the elevated contents of silicon and manganese on the operating characteristics of high-strength wheel steel, Materials Science, 55 (2019) 143–151. https://doi.org/10.1007/s11003-019-00281-4

[23] T. Davey, N. D. Tran, A. Saengdeejing, Y. Chen, First-principles-only CALPHAD phase diagram of the solid aluminium-nickel (Al-Ni) system, Calphad, 71 (2020) 102008. https://doi.org/10.1016/j.calphad.2020.102008

[24] W. Shao, J. M. Guevara-Vela, A. Fernández-Caballero, S. Liu, J. Lorca, Accurate prediction of the solid-state region of the Ni-Al phase diagram including configurational and vibrational entropy and magnetic effects, Acta Materialia, 253 (2023) 118962. https://doi.org/10.1016/j.actamat.2023.118962

[25] J. Romanowska, J. Morgiel, M. Zagula-Yavorska, J. Sieniawski, Nanoparticles in hafnium-doped aluminide coatings, Materials Letters, 145 (2015) 162-166. https:// doi.org/10.1016/j.matlet.2015.01.089

[26] M. Zagula-Yavorska, M. Pytel, J. Romanowska, J. Sieniawski, The effect of zirconium addition on the oxidation resistance of aluminide coatings, Journal of Materials Engineering and Performance, 24 (2015) 1614-1625. https://doi.org/10.1007/s11665-015-1421-5

[27] J. Romanowska, E. Dryzek, J. Morgiel, K. Siemek, Ł. Kolek, M. Zagula-Yavorska, Microstructure and positron lifetimes of zirconium modified aluminide coatings, Archives of Civil and Mechanical

Engineering, 18 (2018) 1150-1155. https://doi.org/10.1016/j.acme.2018.03.002

[28] R. Pillai, A. Chyrkin, D. Grüner, W. Nowak, N. Zheng, A. Kliewe, et al., Carbides in an aluminised single crystal superalloy: Tracing the source of carbon, Surface and Coating Technology, 288 (2016) 15–24. https://doi.org/10.1016/j.surfcoat.2015.12.066

[29] P. Kiruthika, S. K. Makineni, C. Srivastava, K. Chattopadhyay, A. Paul, Growth mechanism of the interdiffusion zone between platinum modified bond coats and single crystal superalloys, Acta Materialia, 105 (2016) 438-448. https://doi.org/10.1016/j.actamat.2015.12.014

[30] H. Meininger, T. Gödeke, M. Ellner, Structural and phase equilibria investigations in the transition metal-rich part of the ternary system Ni–Pd–Al, International Journal of Materials Research, 90 (1999) 207-215. https://doi.org/10.1515/ijmr-1999-900307

[31] M. Bai Fabrication and characterization of thermal barrier coatings. Doctor Thesis. University of Manchester, 182.

[32] P. Lamesle, P. Steinmetz, J. Steinmetz, Palladium-modified aluminide coatings: mechanisms of formation, Journal of Electrochemical Society, 142 (1995) 497-505. https://doi.org/10.1149/1.2044085

[33] Q. Fan, H. Yu, T. Wang, Z. Wu, Y. Liu, Preparation and isothermal oxidation behavior of Zr-doped, Pt-modified aluminide coating prepared by a hybrid process, Coatings, 8 (2018) 1–12. https://doi.org/10.3390/coatings8010001

SINERGIJSKI EFEKAT Pd+Rh NA MIKROSTRUKTURNE OSOBINE I OTPORNOST NA OKSIDACIJU ALUMINIDNIH PREVLAKA

M. Zagula-Yavorska

Univerzitet za tehnologiju u Žešovu, Odsek za nauku o materijalima, Fakultet za mašinstvo i aeronautiku, Žešov, Poljska

Apstrakt

Pd+Rh modifikovane aluminidne prevlake su deponovane na niklu i nikl superleguri CMSX-4. Pd sloj (debljine 2,5 μm), zajedno sa Rh slojem (debljine 0,5 μm), elektrohemijski su naneseni na obe legure. Aluminizacija supstrata sa Pd+Rh slojevima izvršena je CVD metodom. Na obe prevlake primećene su dve zone (spoljna i međudifuziona). Faza β-NiAl s primesama paladijuma formirala se u spoljnim zonama, dok su na granici između spoljne i međudifuzione zone obe prevlake formirane faze β-NiAl s primesama paladijuma i rodijuma. U međudifuzionoj zoni na niklu i superleguri CMSX-4 pronađene su faza γ'-Ni$_3$Al i precipitati μ-Co$_7$Mo$_6$ u matrici β-NiAl. Simultana upotreba Pd i Rh u aluminidnoj prevlaci usporila je brzinu oksidacije, a dodatno, Pd+Rh ko-dopiranje pokazalo se efikasnijim u smanjenju brzine oksidacije aluminidne prevlake na superleguri CMSX-4 u poređenju sa Pd+Hf.

Ključne reči: *Pd+Rh; Aluminidna prevlaka; Oksidacija; Vrednost k$_p$*